Structure Shape Evolution in Lanthanide and Actinide Nuclei

Khalaf A.M.* and Ismail A.M.†

*Physics Department, Faculty of Science, Al-Azhar University, Cairo, Egypt. E-mail: ali_khalaf43@hotmail.com
†Hot Laboratories Center, Atomic Energy Authority, Egypt, P.No. 13759, Cairo, Egypt. E-mail: ahmedismailph@yahoo.com

To give the characteristics of the evolution of the collectivity in even-even nuclei, we studied the behavior of the energy ratios R(4/2) and R(6/4). All chains of lanthanides begins as vibrational with R(4/2) near 2.0 and move towards rotational (R(4/2) $\longrightarrow$ 3.33) as neutron number increases. A rabid jump in R(4/2) near N=90 was seen. The plot of R(4/2) against Z shows not only the existence of a shape transitions but also the change in curvature in the data for N=88 and 90, concave to convex. For intermediate structure the slopes in E-GOS (E_γ over spin) plots range between the vibrator and rotor extremes. The abnormal behavior of the two-neutron separation energies of our lanthanide nuclei as a function of neutron number around neutron number 90 is calculated. Nonlinear behavior is observed which indicate that shape phase transition is occurred in this region. The calculated reduced B(E2) transition probabilities of the low states of the ground state band in the nuclei ^{150}Nd/^{152}Sm/^{154}Gd/^{156}Dy are analyzed and compared to the prediction of vibrational U(5) and rotational SU(3) limits of interacting boson model calculations.

1 Introduction

The interacting boson model (IBM) [1, 2] and the geometric collective model (GCM) [3–5] represent two major phenomenological approaches that successfully describe nuclear collectivity. While the IBM model is purely algebraic, based on a bosonized form of the many-body problem with even numbers of fermions, the GCM model follows from a geometric description of nuclei using the Bohr-Mottelson (BM) Hamiltonian [6].

Quantum phase transitions are of great interest in many areas of physics, and their manifestations vary significantly in different systems. For nuclear systems, the IBM reveals rich features of their shape phase transitions [7–16]. Three dynamical symmetries in the IBM were shown to correspond to three typical shape phase of nuclei, known as the spherical U(5) symmetry, axially deformed SU(3) symmetry and γ-soft deformed O(6) symmetry shapes. It is also known that phase transitions coincide with transitions between dynamical symmetries, with a first order phase transition taking place in the U(5)-SU(3) transition, and a second order phase transition happening in the U(5)-O(6).

A new class of symmetries that applies to systems localized at the critical points was proposed. In particular the critical symmetry E(5) [17] has been suggested to describe critical points in the phase transition from spherical vibrator U(5) to γ-unstable rotor O(6) shapes, while X(5) [18] is designed to describe systems lying at the critical point in the transition from spherical to axially deformed systems. These are based originally on particular solutions of the Bohr-Mottelson differential equations, but are usually applied in the context of the IBM [1], since the IBM provides a simple but detailed framework in which first and second order phase transitions can be studied. In the IBM language, the symmetry E(5) corresponds to the critical point between U(5) and O(6) symmetry limits, while X(5) symmetry should describe the phase transition region between the U(5) and the SU(3) dynamical symmetries.

The purpose of this paper is to disuse the main concepts of the rapid changes in structure of lanthanide and actinide nuclei by using some good indicators like energy ratios, two-neutron separation energies and reduced electric quadruple transition probabilities.

2 Energy Ratios and Nuclear Shape Transition

Nuclear shape phases are the manifestation of the collective motion modes of nuclei. One of the best signatures of shape transition is the behavior of the ratio between the energies of the first 4^+ and 2^+ states

$$R(4/2) = \frac{E(4_1^+)}{E(2_1^+)} \tag{1}$$

along the isotopic chain. The members of vibrational nuclei have excitation energies

$$E(I) = C(I), \tag{2}$$

where C is the vibrational constant. So that the energy ratios are

$$R((I+2)/I)_{vib} = \frac{I+2}{I}. \tag{3}$$

The yrast energies of the harmonic vibrator can be written as

$$E(I) = nE(2_1^+), \tag{4}$$

where n is the phonon number. The γ-ray energies within the yrast band are given by

$$\begin{aligned} E_\gamma(I) &= E(I) - E(I-2) \\ &= E(2_1^+). \end{aligned} \tag{5}$$

It is interesting to discuss the energy levels by plotting the ratio of E_γ(I) to spin I (E-Gamma Over Spin) (E-GOS) [19] against spin I. This is not helpful to identify the structure of the nucleus, but also to discern changes as a function of spin. Therefore, the E-GOS for vibrational nuclei can be written as

$$(E_\gamma/I)_{vib} = E(2_1^+)/I \tag{6}$$

which decreases hyperbolically from $E(2_1^+)/2$ to zero. In the rigid rotor, the energies of the yrast states are:

$$E(I) = AI(I+1), \tag{7}$$

where A is the rotational parameter ($A = \hbar^2/2J$, where J represents the moment of inertia), so that the energy ratios are

$$R((I+2/I))_{rot} = \frac{(I+2)(I+3)}{I(I+1)}. \tag{8}$$

Then The γ-ray energies within the yrast band are given by

$$E_\gamma(I) = A(4I-2) \tag{9}$$

and so the E-GOS is

$$\begin{aligned}(E_\gamma/I)_{rot} &= A\left(4-\frac{2}{I}\right)\\ &= \frac{E(2_1^+)}{3}\left(2-\frac{1}{I}\right).\end{aligned} \tag{10}$$

In units of A, this evolves from 3 for I=2 up to 4 for high I, and so gradually increasing and asymptotic function of I. Also E-GOS for γ-unstable nuclei is given by

$$(E_\gamma/I)_{\gamma-soft} = \frac{E(2_1^+)}{4}\left(1+\frac{2}{I}\right). \tag{11}$$

The R(4/2) varies from the value which correspond to vibrations around a spherical shape of vibrational nuclide R(4/2)=2 to the characteristic value for excitations of well-deformed rotor R(4/2)=3.33. That is, the energy ratio R(4/2) exhibits sharp change in rapid transitional region. Even-even nuclei can be classified roughly according to ratios R(4/2) as:

$1.0 < R(4/2) < 2.0$	for magic nuclei,
$2.0 < R(4/2) < 2.4$	for vibrational nuclei,
$2.4 < R(4/2) < 2.7$	for γ-unstable nuclei,
$2.7 < R(4/2) < 3.0$	for transitional nuclei,
$3.00 < R(4/2) < 3.33$	for rotational nuclei.

To give the characteristics of the evolution of the collectivity in even-even nuclei, we study the behavior of the energy ratios R(4/2) and R(6/4). For the nuclei included in our study, all chains of lanthanides begins as vibrational with R(4/2) near 2.0 and move towards rotational (R(4/2)$\longrightarrow$3.33) as neutron number increases. For intermediate structure the slopes in E-GOS plots range between the vibrator and rotor extremes. One particular case of interest is R(4/2)=3.0 which traditionally marks the boundary where axial rotation begins to set in. A very general phenomenological model is that of the an harmonic vibrator (AHV) [20]. In this model the yrast energies are given by

$$E(I=2n) = nE(2_1^+)\frac{n(n-1)}{2}\epsilon_4, \tag{12}$$

where

$$\epsilon_4 = E(4_1^+) - 2E(2_1^+) \tag{13}$$

is the an harmonically of the 4^+ state, that is, its deviation in energy from twice the 2^+ energy, and n = I/2, n is the phonon number in a vibrational nucleus. For $\epsilon_4 = 0$ equation (12) gives the harmonic vibrator

$$E(I) = \frac{1}{2}E(2_1^+)I \quad (R(4/2) = 2). \tag{14}$$

For $\epsilon_4 = (4/3)E(2_1^+)$, it gives the rigid rotor expression

$$E(I) = \frac{1}{6}E(2_1^+)I(I+1) \quad (R(4/2) = 10/3). \tag{15}$$

For $\epsilon_4 = E(2_1^+)$, it gives

$$E(I) = \frac{1}{8}E(2_1^+)I(I+2) \quad (R(4/2) = 3.0). \tag{16}$$

E(I)/I is constant and that the E-GOS plots is flat. So, interestingly the phase transition point (R(4/2) 3.0) roughly serves to section E-GOS plots into two classes of increasing and decreasing with I, so that nuclei on the vibrator side of the phase transition are down-sloping while these to the rotor side are up-sloping.

The systematics of energy ratios of successive levels of collective bands in medium and heavy mass even-even nuclei were studied [21]. A measure of their deviation from the vibrational and rotational limiting value was found to have different magnitude and spin dependence in vibrational, rotational and γ-unstable nuclei. For a given band for each spin I, the following ratios were constructed to define the symmetry for the excited band of even-even nuclei

$$\begin{aligned}r((I+2)/I) &= \frac{R((I+2)/I)_{exp} - R((I+2)/I)_{vib}}{R((I+2)/I)_{rot} - R((I+2)/I)_{vib}}\\ &= \frac{R((I+2)/I)_{exp} - (I+2)/I}{\dfrac{2(I+2)}{I(I+1)}},\end{aligned} \tag{17}$$

where $R((I+2)/I)_{exp}$ is the experimental value of the ratio. In equation (17), the value of energy ratios, r have changed between 0.1 and 1 for yrast bands of even-even nuclei. The ratio r should be close to one for a rotational nucleus and close to zero for a vibrational nucleus, while it should have intermediate values for γ-unstable nuclei:

$0.10 \le r \le 0.35$	for vibrational nuclei,
$0.4 \le r \le 0.6$	for transitional nuclei,
$0.6 \le r \le 1.0$	for rotational nuclei.

3 Electromagnetic Transition Strengths

When the nucleus is deformed it acquires an electric-multiple moment. Consequently as it oscillates, in $\lambda\mu$ mode, it emits electric $\lambda\mu$ radiation. Now to calculate the radiative transition rates between vibrational states, we need the nuclear electric multiple operator $\hat{\mathcal{M}}$. This is given by

$$\hat{\mathcal{M}}(E\lambda,\mu) = \int_{\tau} d\tau \rho_c(r) r^{\lambda} Y_{\lambda\mu}(\theta,\phi), \tag{18}$$

$\rho_c(r)$ is the charge density of the nucleus. The electric multipole moment is defined by $\hat{Q}_\lambda$

$$\hat{Q}_\lambda = \left(\frac{16\pi}{2\lambda+1}\right)^{1/2} \mathcal{M}(E\lambda,0). \tag{19}$$

We now discuss the electric quadruple moment ($\lambda = 2$) in more detail because the electric quadruple moment Q_2 of a nucleus is a measure of the deviation of the charge distribution from spherical symmetry. We define the reduced transition probability as:

$$\begin{aligned} B(E2, I_i \longrightarrow I_f) &= \textstyle\sum_{Mf} |\langle I_i M_i | Q_2 | I_f M_f\rangle|^2 \\ &= \tfrac{1}{2I_i+1} |\langle I_i \| Q_2 \| I_f\rangle|^2, \end{aligned} \tag{20}$$

where $|\langle I_i \| Q_2 \| I_f\rangle|$ is a reduced matrix element defined by the Wigner-Eckart theorem

$$\langle I_i M_i | \mathcal{M}(E\lambda,\mu) | I_f M_f\rangle| = \langle I_i M_i \lambda\mu | I_f M_f\rangle \frac{|\langle I_i \| \mathcal{M}(E\lambda) \| I_f\rangle|}{(2I_i+1)^{1/2}}.$$

The reduced transition probability $B(E2, I_i K \longrightarrow I_f K)$ for an electric quadruple transition between two members of same rotational band with quantum number K is:

$$B(E2, I_i K \longrightarrow I_f K) = \frac{5}{16\pi} e^2 Q_0^2 \langle I_i K 20 | I_f K\rangle^2, \tag{21}$$

where Q_0 is the transition intrinsic quadruple moment and we have used

$$\sum_{m_1 m_2, m} |\langle I_1 m_1 I_2 m_2 | I m\rangle|^2 = 2I + 1. \tag{22}$$

For even-even nuclei, $K = 0$ and when $I_i = I$ and $I_f = I-2$, we get the familiar relations between $B(E2, I \longrightarrow I-2)$ and the intrinsic quadruple moment Q_0 are:

$$B(E2, I \longrightarrow I-2) = \frac{5}{16\pi} e^2 Q_0^2 \frac{3}{2} \frac{I(I-1)}{2(2I-1)(2I+1)}. \tag{23}$$

As a special case for the transition $2^+ \longrightarrow 0^+$, yields

$$B(E2, 2^+ \longrightarrow 0^+) = \frac{5}{16\pi} e^2 Q_0^2. \tag{24}$$

For the transition $I_i = I$ and $I_f = I+2$, yields

$$B(E2, I \longrightarrow I+2) = \frac{5}{16\pi} e^2 Q_0^2 \frac{3}{2} \frac{(I+2)(I+1)}{2(2I+1)(2I+2)} \tag{25}$$

and for special case for the transition $0^+ \longrightarrow 2^+$, yields

$$B(E2, 0^+ \longrightarrow 2^+) = \frac{5}{16\pi} e^2 Q_0^2. \tag{26}$$

That is

$$B(E2, 2^+ \longrightarrow 0^+) = 0.2\, B(E2, 0^+ \longrightarrow 2^+). \tag{27}$$

From equation (21), the intrinsic quadruple moment Q_0 for a $K = 0$ band of an axially symmetric rotor is extracted. For the special transition $0^+ \longrightarrow 2^+$, we get

$$eQ_0 = \left[\frac{16\pi}{5} B(E2, 0^+ \longrightarrow 2^+)\right]^{1/2} \tag{28}$$

in units of 10^{-24} cm^2.

The electric reduced transition probability $B(E\lambda)$ can be obtained from the transition probability per unit time for emission of photon of energy $\hbar\omega$, angular momentum λ and of electric type with the nucleus going from a state i to a state f defined by

$$T(E\lambda) = \frac{8\pi(\lambda+1)}{\lambda[(2\lambda+1)!!]^2} \frac{1}{\hbar} \left(\frac{E_\gamma}{\hbar c}\right)^{(2\lambda+1)}. \tag{29}$$

$T(E\lambda)$ for electric quadruple has the from

$$T(E2) = \frac{4\pi}{75} \frac{1}{\hbar} \left(\frac{E_\gamma}{\hbar c}\right)^5 B(E2). \tag{30}$$

For the quadruple transition $T(E2)$ can be derived experimentally from the relation

$$T(E2, 2^+ \longrightarrow 0^+) = \frac{ln2}{(1+\alpha)\tau_{1/2}}, \tag{31}$$

where α is the total conversion coefficient taken from the tabulated values given by Rose [22] and $\tau_{1/2}$ is the half life time. From equations (30) and (31), one can find $B(E2)$:

$$\begin{aligned} B(E2, 2^+ \longrightarrow 0^+) &= \frac{75\hbar}{4\pi} \left(\frac{\hbar c}{E_{2^+}}\right)^5 \frac{ln2}{(1+\alpha)\tau_{1/2}} \\ &= 0.565502 \left(\frac{100}{E_{2^+}}\right)^5 \frac{1}{(1+\alpha)\tau_{1/2}}, \end{aligned} \tag{32}$$

where $B(E2)$ is in units of e^2b^2 when E_{2^+} is in units of MeV and $\tau_{1/2}$ in units of nanosecond.

4 The two–neutron Separation Energies

The energy required to remove a neutron from a nucleus with Z proton and N neutron is called separation energy and is defined as:

$$S_n(Z,N) = [M(Z,N-1) + M_n - M(Z,N)]C^2. \tag{33}$$

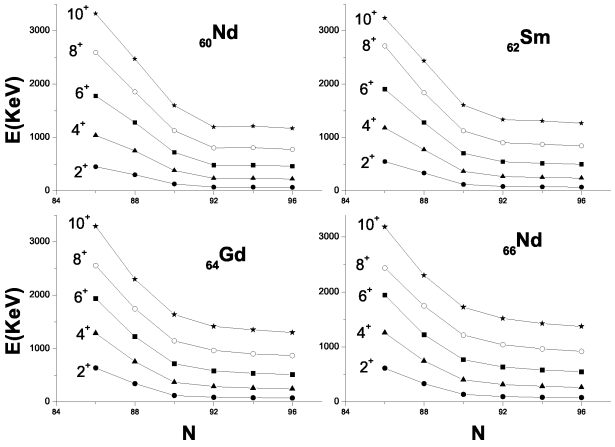

Fig. 1: Systematics of low-lying yrast level energies in even-even lanthanides Nd/Sm/Gd/Dy isotopes. The 2^+, 4^+, ..., 10^+ level energies are plotted. The states are labeled by I^π.

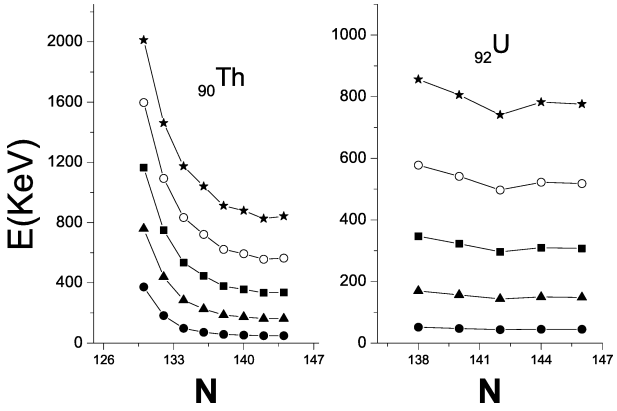

Fig. 2: The same as Fig. (1) but for actinides Th/U isotopes.

This expression can be rewritten in the form of binding energy as:

$$S_n(Z,N) = B(Z,N) - B(Z,N-1). \quad (34)$$

The definition of the two-neutron separation energies is the following:

$$S_{2n} = B(N) - B(N-1), \quad (35)$$

where N denotes the number of valence nucleon pairs and it is assumed that we are treating nuclei belonging to the first half of the neutron shell (50 - 82) filling up with increasing mass number.

5 Numerical Calculations and Discussions

The systematics of the excitation energies of the low-lying states as a function of neutron number changing from 84 to 100 in the even-even lanthanides Nd/Sm/Gd/Dy isotopes in the mass region 144–166 and the actinide Th/U isotopes in the mass region 224–238 are presented in Figures (1,2). Only the yrast state of positive parity and spin $I^\pi = 2^+, 4^+, 6^+, 8^+$ and 10^+ has been included.

The trend of increasing excitation energy of 2^+ state with decreasing neutron number, implying a corresponding fall in deformation as the N = 82 shell closure is approached. The energies of the 4^+ and 6^+ states also display the same trend. For lanthanides isotopes we can see that the energy values for each spin I states change almost linearly for $N \leq 88$ and become quite flat for $N \geq 90$. This is consistent with the onset of the Z = 64 sub-shell effect. Furthermore, the linear falling of the energy value for each I state as N goes from 86 to 88 seems to justify the linear variation of the effective proton-boson number in each isotope series.

As an example Figure (1) shows that the limits (spherical shape and well deformed rotor) are fulfilled in the Neodymium ^{144}Nd and $^{152-156}$Nd isotopes respectively, and also that there is a smooth transition between them. The ^{148}Nd isotopes could be considered as a transitional nucleus in the calculations. A rapid rise in R(4/2) between N = 88 and 90 is shown, where it increases from values of ≃2.3 typical of actual vibrational nuclei to 3.0, the traditional borderline value separating spherical from deformed nuclei to ≃3.3 the limiting value of the axial rotor model. As a matter of fact, if we compare the X(5) results (first order phase transition from a spherical vibrator to an axially deformed rotor is called X(5)) with the energy levels in ^{148}Nd, we find striking similarities, it suggested that the nucleus ^{148}Nd display the X(5) symmetry.

The nature of the low-lying states in our lanthanides and actinides chains of isotopes can be illustrated in Figures (3,4) by examining the ratios of the excitation energies R(4/2) and R(6/4) as a function of neutron number. The limiting values for R(4/2) and R(6/4) for harmonic vibrator are 2.0 and 1.5 and for rigid symmetric rotor are 0.33 and 2.1 respectively.

In lanthanides the calculated values increases gradually from vibrational value to transitional value near N=90 to rotor

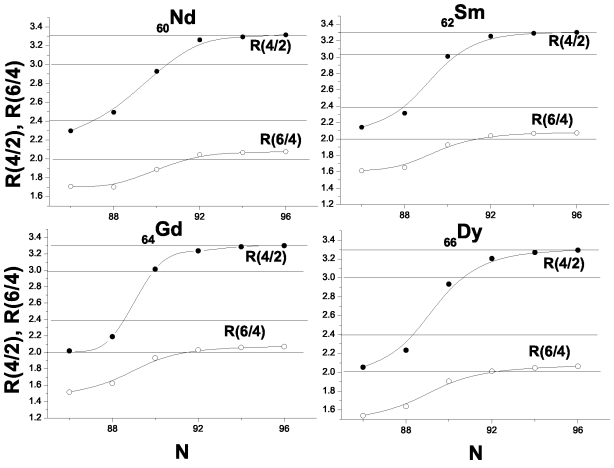

Fig. 3: Evolution of energy ratios R(4/2) and R(6/4) for lanthanides Nd/Sm/Gd/Dy isotopes as function of increasing neutron number.

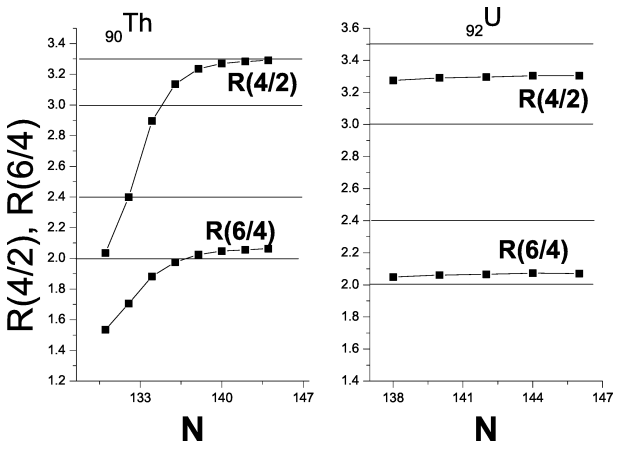

Fig. 4: The same as Fig. (3) but for actinides Th/U isotopes.

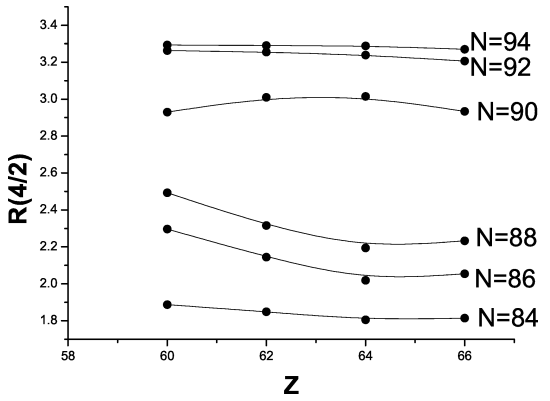

Fig. 5: The plot of R(4/2) values in the Nd/Sm/Gd/Dy region against Z. We see change in curvature in the data for N=88 and N=90 concave to convex.

value in the heavier isotopes. The energy ratios R(4/2) and R(6/4) for even A, N=88 isotopes are essentially constant for Sm, Gd and Dy.

The same data for lanthanides is plotted between R(4/2) against Z instead of N, see Figure (5). We see a rapid jump in R(4/2) near N=90. Here, the plot of R(4/2) against Z shows not only the existence of a shape transitions but also the change in curvature in the data for N=88 and 90, concave to convex. For Gd nuclei for N≤88 the behavior is typically closed shell, while for $N \geq 90$ the behavior appears to be near mid shell.

The nuclei of lanthanides region would therefore be candidates for a shape transition from vibrator to axially rotator and the N = 90 isotopes ^{150}Nd, ^{152}Sm, ^{154}Gd and ^{156}Dy are ideal candidates for X(5). Historically, sensitive studies [23] of the ^{152}Sm level scheme led to a suggestion that this nucleus gave evidence for a first order phase transition [24], its R(4/2) value is intermediate between vibrator and rotor [25]. Additional X(5) candidate in the lanthanides region have subsequently been identified in ^{150}Nd [26], ^{154}Gd [27], ^{156}Dy [28] and ^{162}Yb [29]. Fig. (6) shows R(I/2) and E-GOS plots for a vibrator, a rotor and R(4/2)=3 modes.

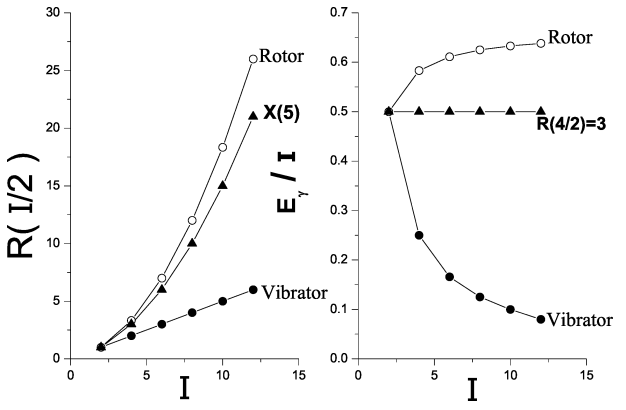

Fig. 6: Comparison of R(I/2) and E-GOS plots for three kinds of collective modes vibrator, rotor and R(4/2)=3 modes.

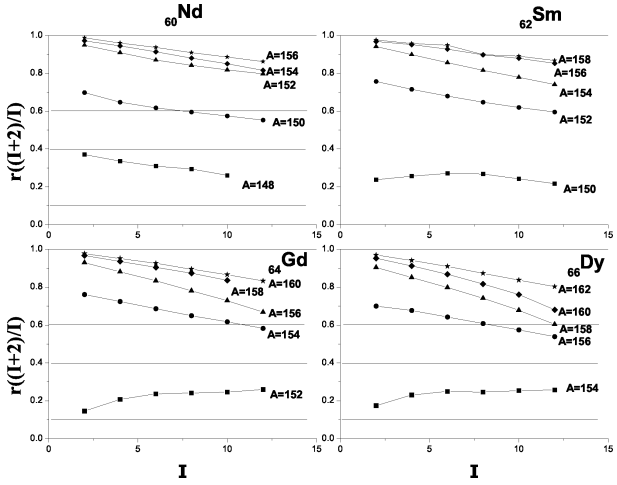

Fig. 7: The $r((I+2)/I)$ energy ratios for the ground state bands of even-even Lanthanides Nd/Sm/Gd/Dy isotopes as a function of spin I.

To investigate the dependence of energy ratios on the angular momentum, the useful criterion r((I + 2)/I) are examined for distinguishing between different kinds of collective behavior. In Figures (7,8) we show the results of our calculations for the ground state bands of the selected lanthanides and actinides isotopes. The study supports the interpretation of ^{150}Nd and ^{152}Sm as a critical point nucleus. Hence, the isotopes ^{150}Nd and ^{152}Sm are associated to X(5) symmetry. For the vibrational nuclei ^{152}Gd and ^{154}Dy, the ratios r((I + 2)/I) start with a small value and then increases with I, more rapidly in the beginning and slower at higher I's. On the other hand for rotational nucleus ^{162}Dy the ratios r((I + 2)/I) start with a value very close to one and then constantly decrease.

As an example, the abnormal behavior of the two-neutron

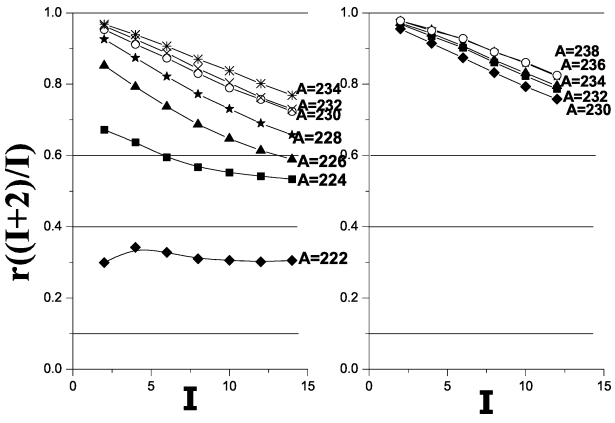

Fig. 8: The same as Fig. (7) but for Actinides Th/U isotopes.

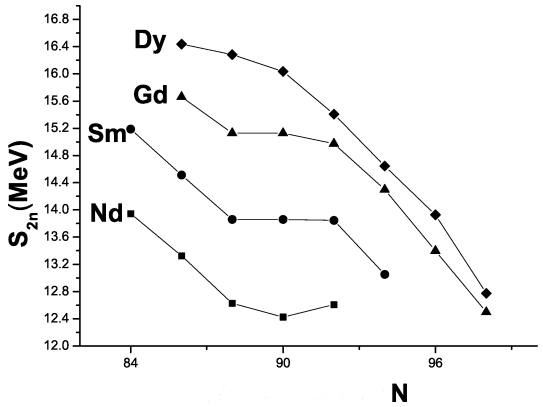

Fig. 9: Two-neutron separation energies S_{2n} for the chains Nd/Sm/Gd/Dy isotopes as a function of the number of neutrons.

separation energies S_{2n} of nuclei Nd/Sm/Gd/Dy as a function of neutron number around neutron number 90 is illustrated in Fig. (9), the nonlinear behavior of S_{2n} indicates that shape phase transition may occur in this region. It is commonly assumed that the ratio of the B(E2) reduced transition probabilities between the levels of the ground state band takes the values between vibrational and rotational limits. In the interacting boson model IBM [1] both these limits are corrected because the number of the quadruple bosons cannot exceed some maximum value N.

In the U(5) vibrational limit of IBM,

$$\frac{B(E2, I+2 \to I)}{B(E2, 2^+ \to 0^+)} = \frac{1}{2}(I+2)\left(1-\frac{1}{2N}\right)$$

and in the SU(3) rotational limit of IBM,

$$\frac{B(E2, I{+}2 \to I)}{B(E2, 2^+ \to 0^+)} = \frac{15}{2}\left(1{-}\frac{1}{2N}\right)\left(1{-}\frac{1}{2N{+}3}\right)\frac{(I{+}2)(I{+}1)}{(2I{+}3)(2I{+}5)}.$$

Our GCM calculated values of these ratios are put between these limits, *i.e.*, the IBM calculations can reproduce the E2 transition probabilities.

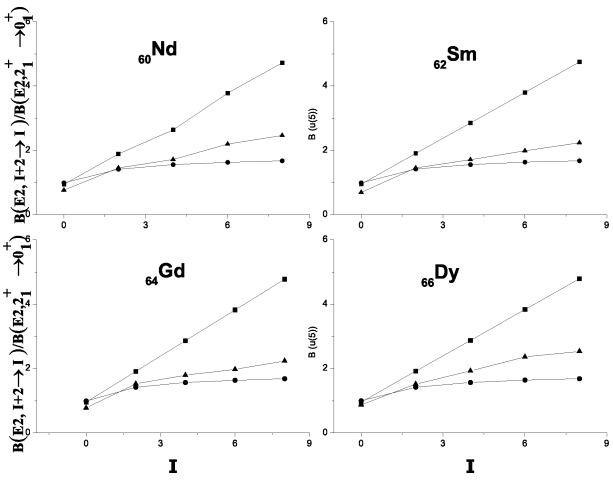

Fig. 10: The ratio $\frac{dB(E2,I+2\longrightarrow I)}{B(E2,2^+\longrightarrow 0^+}$ of reduced transition probabilities between the levels of the ground state band of ^{150}Nd, ^{152}Sm, ^{154}Gd and ^{156}Dy as compared to the U(5) and SU(3) of IBM calculations (• for U(5), ∘ for SU(3) and x for present calculation).

Table 1: The GCM parameters as derived in fitting procedure used in the calculation.

Nucleus	I	U(5) Vibrator	SU(3) Rotor	Present calculations
^{150}Nd (N=9)	0	0.94444	0.98941	0.75812
	2	1.88888	1.41345	1.45375
	4	2.63333	1.55677	1.71683
	6	3.77777	1.62962	2.19186
	8	4.72222	1.67381	2.46675
^{152}Sm (N=10)	0	0.95	0.99130	0.68900
	2	1.90	1.41614	1.45137
	4	2.85	1.55973	1.71262
	6	3.80	1.63272	1.98838
	8	4.75	1.67700	2.23512
^{154}Gd (N=11)	0	0.95454	0.99272	0.77300
	2	1.90909	1.41818	1.52393
	4	2.86363	1.56197	1.79560
	6	3.81818	1.63507	1.97412
	8	4.77272	1.67941	2.23803
^{156}Dy (N=12)	0	0.95833	0.99382	0.87381
	2	1.91666	1.41975	1.51345
	4	2.87500	1.56370	1.92725
	6	3.83333	1.63688	2.35673
	8	4.79166	1.68127	2.53512

The calculated $B(E2, I+2 \longrightarrow I)/B(E2, 2^+ \longrightarrow 0^+)$ ratios using GCM for the ground state bands of the low-lying state are presented in Table (1) and Fig. (10) together with

the results for the vibrator and rotor limits of IBM for ^{150}Nd, ^{152}Sm, ^{154}Gd and ^{156}Dy.

Submitted on January 15, 2013 / Accepted on January 21, 2013

References

1. Iachello F. and Arima A. The Interacting Boson Model. Cambridge University Press, Cambridge, England, 1987.
2. Frank A. and VanIsacker P. Algebraic Methods in Molecular and Nuclear Structure Physics. Wiley, New York, 1994.
3. Eisenberg J. and Greiner W. Nuclear Theory, Vol. I, Nuclear Models: Collective and Single-Particle Phenomena. North-Holland, Amsterdam, 1987.
4. Troltenier D., Hess P.O. and Maruhn J. Computational Nuclear Physics, Vol. I, Nuclear Structure. Springer, Berlin, Heidelberg, New York, 1991.
5. Troltenier D. Das Generalisierte Kollektivmodell. Frankfurt am Main, Germany, Report No. GSI-92-15, 1992.
6. Bohr A. and Mottelson. Nuclear Structure v. II. Benjamin, New York, 1975.
7. Jolie J. et al. Two-Level Interacting Boson Models Beyond The Mean Field. *Physical Reveiw*, 2007, v. C75, 014301R–014310R.
8. Iachello F. and Zamfir N.V. Quantum Phase Transitions in Mesoscopic Systems. *Physical Review Letters*, 2004, v. 92(3), 212501–212504.
9. Cejnar P., Heinze S. and Dobes J. Thermodynamic Analogy for Quantum Phase Transitions at Zero Temperature. *Physical Review*, 2005, v. C71, 011304R–011309R.
10. Rowe D.J. Quasi Dynamical Symmetry in an Interacting Boson Model Phase Transition. *Physical Review Letters*, 2004, v. 93, 122502–122505.
11. Liu Y.X., Mu L.Z. and Wei H. Approach to The Rotation Driven Vibrational to Axially Rotational Shape Phase Transition Along The Yrast Line of a Nucleus. *Physics Letters*, 2006, v. B633, 49–53.
12. Zhang Y., Hau Z. and Liu Y.X. Distinguishing a First Order From a Second Order Nuclear Shape Phase Transition in The Interacting Boson Model. *Physical Review*, 2007, v. C76, 011305R–011308R.
13. Arios J.M., Dukelsky J. and Garcia-Ramos J.E. Quantum Phase Transitions in the Interacting Boson Model: Integrability, Level Repulsion and Level Crossing. *Physical Review Letters*, 2003, v. 91, 162502–162504.
14. Garcia-Ramos J.E. et al. Two-Neutron Separation Energies, Binding Energies and Phase Transitions in The Interacting Boson Model. *Nuclear Physics*, 2001, v. A688, 735–754.
15. Liu M.L. Nuclear Shape-Phase Diagrams. *Physical Review*, 2007, v. C76, 054304–054307.
16. Heyde K. et al. Phase Transitions Versus Shape Coexistence. *Physical Review*, 2004, v. C69, 054304–054309.
17. Iachello F. Dynamic Symmetrcies at The Critical Point. *Physical Review Letters*, 2000, v. 85, 3580–3583.
18. Iachello F. Analytic Prescription of Critical Point Nuclei in a Spherical Axially Deformed Shape Phase Transtion. *Physical Review Letters*, 2001, v. 87, 052502–052506.
19. Regan P.H. et al. Signature for Vibrational to Rotational Evolution Along the Yrast Line. *Physical Review Letters*, 2003, v. 90, 152502–152505.
20. Zamfir N.V. et al. Study of Low-Spin States in ^{122}Cd. *Physical Review*, 1995, v. C51, 98–102.
21. Bonatsos D. and Skoures L.D. Successive Energy Ratios in Medium- and Heavy-Mass Nuclei as Indicators of Different Kinds of Collectivity. *Physical Review*, 1991, v. C43, 952R–956R.
22. Rose M.E. Internal Conversion Coefficients. Amsterdam, North Holland . North-Holland, Publishing Company 1958.
23. Casten R.F. The First Excited 0^+ State in ^{152}Sm. *Physical Review*, 1998, v. C57, 1553R–1557R.
24. Casten R.F. Kusnezov D. and Zamfir N.V. Phase Transitions in Finite Nuclei and The Integer Nucleon Number Problem. *Physical Review Letters*, 1999, v. 82, 5000–5003.
25. Clark R.M. et al. Searching For X(5) Behavior in Nuclei. *Physical Review*, 2003, v. C68, 037301–037304.
26. Krücken R. et al. B(E2) Values in ^{150}Nd and The Critical Point Symmetry X(5). *Physical Review Letters*, 2002, v. 88, 232501–232501.
27. Tonev D. et al. Transition Probabilities in ^{154}Gd: Evidence for X(5) Critical Point Symmetry. *Physical Review*, 2004, v. C69, 034334–034339.
28. Caprio M.A. et al. Low-Spin Structure of 156Dy Through γ-ray Spectroscopy. *Physical Review*, 2002, v. C66, 054310–054328.
29. McCutchan E.A. et al. Low Spin States in ^{162}Yb and The X(5) Critical Point Symmetry. *Physical Review*, 2004, v. C69, 024308–024317.